A Passive Analytical Per-Unit-Length Internal Impedance Matrix Model for Multiconductor Interconnections

Frédéric Broydé and Evelyne Clavelier

Tekcem

Maule, France

e-mail: fredbroyde@tekcem.com, eclavelier@tekcem.com

Abstract — **Based on multiconductor transmission line (MTL) theory, we describe a technique for a simple computation of the high-frequency (h.f.) current distribution in a multiconductor interconnection and of the h.f. per-unit-length (p.u.l.) resistance matrix of the interconnection. This result is used in a model for the p.u.l. internal impedance matrix of the interconnection. We show that this model is passive, hence causal.**

Fig. 1. Cross-section of a multiconductor microstrip interconnection comprising $n = 4$ transmission conductors (TCs) and a reference or ground conductor (GC). The arc length on the perimeter of each TC, denoted by s, is explained and used in Section V.

I. INTRODUCTION

When a researcher wishes to explore possible designs of innovative interface circuits for interconnections built in printed circuit boards or multi-chip modules, he does not need to simulate an actual link comprising vias, packaging parasitics, etc, since no detailed configuration is specified. At this early design stage, it is convenient to use a multiconductor transmission line (MTL) model for the interconnection, usually a uniform MTL model in which the length of the interconnection is easily changed using a single simulation parameter. If the MTL model takes resistive losses into account, it uses a non-zero per-unit-length (p.u.l.) internal impedance matrix, precisely defined below in Section VII.

This paper proposes an analytical model for the p.u.l. internal impedance matrix of a uniform multiconductor interconnection having n transmission conductors (TCs) and a reference or ground conductor (GC), for instance used for signal transmission in a parallel link. The cross-section of such an $(n + 1)$-conductor interconnection is shown in Fig. 1, in the special case of a simple multiconductor microstrip structure. Our model does not take into account characteristics which might occur but are not necessarily present, such as plated conductors (e.g. nickel-plated traces), conductor roughness, anisotropy of a composite substrate, etc.

In sections II to VI of this paper, we want to describe the high-frequency (h.f.) current distribution in the cross-section of the actual interconnection, referred to as "interconnection 1", and to use this result to compute its h.f. p.u.l. resistance matrix. In the case of a two-conductor interconnection (for which $n = 1$), the current distribution is usually computed as the solution of an equation involving the longitudinal electric field or vector potential [1] [2]. In this paper, we consider a different approach, which only applies in the quasi-TEM approximation. However, our approach is easily implemented and fast, even in the case $n \geq 2$. We define an "interconnection 2" as identical to the interconnection 1, except that, in the interconnection 2, the dielectrics are replaced with vacuum and the conductors are replaced with ideal conductors having the same geometry. Section
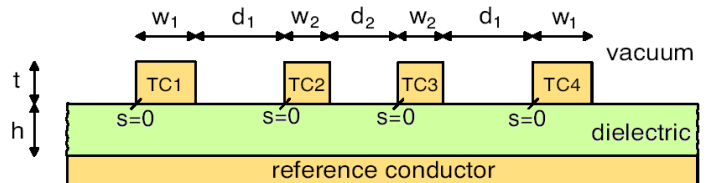
II states some results of electromagnetic theory and MTL theory, applicable to the interconnection 2. In Sections III and IV, we establish general properties of the current and charge distributions in the interconnections 1 and 2. In Sections V and VI, these results are used to derive the h.f. current distribution and the h.f. p.u.l. resistance matrix of the interconnection 1.

The model for the p.u.l. internal impedance matrix is introduced in Section VII. We prove the passivity of this model in Section VIII, which also guaranties that the model is causal [3] [4]. An example of interconnection is treated throughout the paper.

II. LOSSLESS INTERCONNECTION WITHOUT DIELECTRICS

In the interconnection 2 defined in the introduction, we only consider the propagation of TEM waves along the z axis, which takes place at the velocity of light in vacuum, denoted by c_0. The most general frequency domain electric field solution is given by [5, § 9.1] [6, § 3.1]

$$\mathbf{E} = \mathbf{E}_A(x, y) e^{-j\frac{\omega}{c_0}z} + \mathbf{E}_B(x, y) e^{+j\frac{\omega}{c_0}z} \tag{1}$$

where ω is the radian frequency, $\mathbf{E}_A(x, y)$ is a transverse electric field applicable to a wave propagating in the direction of increasing z, and $\mathbf{E}_B(x, y)$ is a transverse electric field applicable to a wave propagating in the direction of decreasing z. The two-dimensional fields $\mathbf{E}_A(x, y)$ and $\mathbf{E}_B(x, y)$ are related to the two-dimensional gradients of the potential functions $\psi_A(x, y)$ and $\psi_B(x, y)$, by $\mathbf{E}_A(x, y) = -\nabla_T \psi_A(x, y)$ and $\mathbf{E}_B(x, y) = -\nabla_T \psi_B(x, y)$, where ∇_T denotes the transverse part of the vector operator ∇. The magnetic field is given by

$$\mathbf{H} = \frac{1}{\eta_0} \mathbf{e}_z \times \left(\mathbf{E}_A(x, y) e^{-j\frac{\omega}{c_0}z} - \mathbf{E}_B(x, y) e^{+j\frac{\omega}{c_0}z} \right) \tag{2}$$

where $\mathbf{e}_z$ denotes the unit vector of the z axis and η_0 is the intrinsic impedance of free-space. The equations (1) and (2) are direct consequences of Maxwell's equations.

According to MTL theory, for any interconnection, the column-vector of the voltages of the TCs with respect to ground, denoted by $\mathbf{V}(z)$, and the column-vector of the currents on the TCs, denoted by $\mathbf{I}(z)$, are given by [7, § 4.3.2] [8]

$$\mathbf{I}(z) = \mathbf{T}\left(e^{-\Gamma z}\mathbf{T}^{-1}\mathbf{I}_A - e^{+\Gamma z}\mathbf{T}^{-1}\mathbf{I}_B\right) \tag{3}$$

$$\mathbf{V}(z) = \mathbf{Z}_C\mathbf{T}\left(e^{-\Gamma z}\mathbf{T}^{-1}\mathbf{I}_A + e^{+\Gamma z}\mathbf{T}^{-1}\mathbf{I}_B\right) \tag{4}$$

where $\mathbf{T}$ is the transition matrix from modal currents to natural currents, Γ is the diagonal matrix of the propagation constants, $\mathbf{Z}_C$ is the characteristic impedance matrix of the MTL and where $\mathbf{I}_A$ and $\mathbf{I}_B$ are column-vectors of currents determined by the configurations at the ends of the interconnection. For the interconnection 2, $\Gamma = (\omega/c_0)\,\mathbf{1}_n$, where $\mathbf{1}_n$ denotes the identity matrix of size $n \times n$, $\mathbf{Z}_C$ is real and we may choose $\mathbf{T} = \mathbf{1}_n$ [7, § 4.4.1]. Thus, we may write

$$\mathbf{V}(z) = \mathbf{V}_A\, e^{-j\frac{\omega}{c_0}z} + \mathbf{V}_B\, e^{+j\frac{\omega}{c_0}z} \tag{5}$$

$$\mathbf{I}(z) = \mathbf{Z}_C^{-1}\left(\mathbf{V}_A\, e^{-j\frac{\omega}{c_0}z} - \mathbf{V}_B\, e^{+j\frac{\omega}{c_0}z}\right) \tag{6}$$

where $\mathbf{V}_A$ and $\mathbf{V}_B$ are column-vectors of voltages determined by the configurations at the ends of the interconnection. Clearly, $\psi_A(x, y)$ is the solution of Laplace's equation $\nabla_T{}^2\psi_A(x, y) = 0$ for the Dirichlet boundary conditions defined by $\mathbf{V}_A$, while $\psi_B(x, y)$ is the solution of Laplace's equation $\nabla_T{}^2\psi_B(x, y) = 0$ for the Dirichlet boundary conditions defined by $\mathbf{V}_B$.

III. Surface Current Density

In the interconnection 2, the surface current density being axial (i.e. parallel to $\mathbf{e}_z$), the axial component of the surface current density on the surface of the conductors is given by

$$j_S = \mathbf{e}_z \cdot \left[\mathbf{n} \times \mathbf{H}(x, y, z)\right] \tag{7}$$

where $\mathbf{n}$ is the unit vector normal to the boundary drawn from the conductor to vacuum. Using (2), we get

$$j_S = \frac{\mathbf{n}}{\eta_0} \cdot \left[\mathbf{E}_A(x,y)e^{-j\frac{\omega}{c_0}z} - \mathbf{E}_B(x,y)e^{+j\frac{\omega}{c_0}z}\right] \tag{8}$$

Let us consider a first configuration where, at a given abscissa $z = z_G$, a column-vector of the currents on the conductors, denoted by $\mathbf{I}(z_G)$, is observed. On the boundary of the conductors, according to (8), we may write

$$j_S = \frac{\mathbf{n}}{\eta_0} \cdot \mathbf{E}_G(x, y) = -\frac{\mathbf{n}}{\eta_0} \cdot \nabla_T\psi_G(x, y) \tag{9}$$

where

$$\mathbf{E}_G(x, y) = \mathbf{E}_A(x, y)e^{-j\frac{\omega}{c_0}z_G} - \mathbf{E}_B(x, y)e^{+j\frac{\omega}{c_0}z_G} \tag{10}$$

and

$$\psi_G(x, y) = \psi_A(x, y)e^{-j\frac{\omega}{c_0}z_G} - \psi_B(x, y)e^{+j\frac{\omega}{c_0}z_G} \tag{11}$$

Here, $\psi_G(x, y)$ is the solution of Laplace's equation $\nabla_T{}^2\psi_G(x, y) = 0$ for the Dirichlet boundary conditions defined by

$$\mathbf{V}_A\, e^{-j\frac{\omega}{c_0}z_G} - \mathbf{V}_B\, e^{+j\frac{\omega}{c_0}z_G} = \mathbf{Z}_C\mathbf{I}(z_G) \tag{12}$$

where we have used (6). Consequently, the surface current density j_S does not depend on the choice of $\mathbf{V}_A$ and $\mathbf{V}_B$ and is uniquely defined by $\mathbf{I}(z_G)$. Clearly, $\psi_G(x, y)$ is a linear function of $\mathbf{I}(z_G)$, but it is otherwise independent of z_G and of frequency. Consequently, at a given (x, y) on the boundary of the conductors at $z = z_G$, using (9), we find that j_S is a linear function of $\mathbf{I}(z_G)$, which may be represented with the matrix $\mathbf{M}(x, y)$ such that

$$j_S(x, y, z_G) = \mathbf{M}(x, y)\mathbf{I}(z_G) \tag{13}$$

where $\mathbf{M}(x, y)$ is frequency-independent and has the dimensions of m^{-1}. Moreover, we observe that, if $\mathbf{I}(z_G)$ is a real vector, $\psi_G(x, y)$ is a real potential function because, in (12), $\mathbf{Z}_C$ is a real matrix. Thus, if $\mathbf{I}(z_G)$ is a real vector, (9) shows that j_S is real, so that $\mathbf{M}(x, y)$ is real.

For the interconnection 1, our reasoning does not apply because (2) and (6) need not be satisfied. Let us assume that resistive losses are small, so that the currents mainly flow close to the surface of the conductors and a surface current density j_S can be considered. No general formula can be used in place of (8) since MTL theory is exactly compatible with Maxwell equations only in the case of an homogeneous medium surrounding perfect conductors. However, in the framework of MTL theory, at each abscissa z, the effects of $\mathbf{I}(z)$, such as the magnetic field and the resulting j_S given by (7), are assumed to be independent from the effects of $\mathbf{V}(z)$, such as the electric field. Thus, for a given $\mathbf{I}(z)$, j_S is unaffected by the presence of dielectrics and we can state the following theorem.
Theorem on the surface current density. At a given abscissa $z = z_G$ of the interconnection 1, for small resistive losses (h.f. current distribution), the surface current density j_S on the boundary of the conductors is given by (13), where $\mathbf{M}(x, y)$ is a real $1 \times n$ matrix which neither depends on the abscissa nor on the frequency.

IV. Surface Charge Density

In the interconnection 2, at the boundary of the conductors, the surface charge density is given by

$$\rho_S = \varepsilon_0\, \mathbf{n} \cdot \left[\mathbf{E}_A(x,y)e^{-j\frac{\omega}{c_0}z} + \mathbf{E}_B(x,y)e^{+j\frac{\omega}{c_0}z}\right] \tag{14}$$

where ε_0 is the permittivity of vacuum. Let us consider a second configuration where, at an abscissa $z = z_H$, a column-vector of the p.u.l. charge density on the boundary of the conductors, denoted by $\mathbf{Q}(z_H)$, is observed. By charge conservation, we have

$$j\omega\,\mathbf{Q}(z_H) = -\frac{d\,\mathbf{I}}{dz}\bigg|_{z_H} \tag{15}$$

Using (5) and (6), we get

$$\mathbf{Q}(z_H) = \frac{\mathbf{Z}_C^{-1}}{c_0}\left(\mathbf{V}_A\, e^{-j\frac{\omega}{c_0}z_H} + \mathbf{V}_B\, e^{+j\frac{\omega}{c_0}z_H}\right) = \frac{\mathbf{Z}_C^{-1}\mathbf{V}(z_H)}{c_0} \quad (16)$$

At $z = z_H$, on the boundary of the conductors, according to (14), we may write

$$\rho_S = \varepsilon_0\, \mathbf{n}\cdot\mathbf{E}_H = -\varepsilon_0\, \mathbf{n}\cdot\nabla_T\psi_H \quad (17)$$

where

$$\mathbf{E}_H(x,y) = \mathbf{E}_A(x,y)\,e^{-j\frac{\omega}{c_0}z_H} + \mathbf{E}_B(x,y)\,e^{+j\frac{\omega}{c_0}z_H} \quad (18)$$

and

$$\psi_H(x,y) = \psi_A(x,y)\,e^{-j\frac{\omega}{c_0}z_H} + \psi_B(x,y)\,e^{+j\frac{\omega}{c_0}z_H} \quad (19)$$

Here, $\psi_H(x, y)$ is the solution of Laplace's equation $\nabla_T^2\psi_H(x, y) = 0$ for the Dirichlet boundary conditions defined by

$$\mathbf{V}_A\, e^{-j\frac{\omega}{c_0}z_H} + \mathbf{V}_B\, e^{+j\frac{\omega}{c_0}z_H} = \mathbf{V}(z_H) = c_0\, \mathbf{Z}_C\mathbf{Q}(z_H) \quad (20)$$

where we have used (16). Thus, the surface charge density ρ_S is uniquely defined by $\mathbf{V}(z_H)$ or equivalently by $\mathbf{Q}(z_H)$. We see that $\psi_H(x, y)$ is a linear function of $\mathbf{Q}(z_H)$, but it is otherwise independent of z_H and of the frequency. Consequently, at a given (x, y) on the boundary of the conductors at $z = z_H$, ρ_S is a linear function of $\mathbf{Q}(z_H)$, which may be represented with the frequency-independent matrix $\mathbf{N}(x, y)$ such that

$$\rho_S(x,y,z_H) = \mathbf{N}(x,y)\mathbf{Q}(z_H) \quad (21)$$

where $\mathbf{N}(x,y)$ has the dimensions of m^{-1}. Additionally, we observe that, if $\mathbf{Q}(z_H)$ is a real vector, $\psi_H(x, y)$ and $\mathbf{V}(z_H)$ are real because $\mathbf{Z}_C$ is a real matrix. Thus, if $\mathbf{Q}(z_H)$ is real, (17) shows that ρ_S is real, so that $\mathbf{N}(x, y)$ is real and describes the electrostatic charge distribution. We have proved a second theorem.

Theorem on the surface charge density. At a given abscissa $z = z_H$ of the interconnection 2, the surface charge density ρ_S on the boundary of the conductors is given by (21), where $\mathbf{N}(x, y)$ is a real $1 \times n$ matrix which neither depends on the abscissa nor on the frequency, $\mathbf{N}(x, y)$ describing the electrostatic charge distribution.

V. HIGH-FREQUENCY CURRENT DISTRIBUTION

We now observe that $\psi_G(x, y)$ and $\psi_H(x, y)$ are the solutions of Laplace's equation for the Dirichlet boundary conditions defined by $\mathbf{Z}_C\,\mathbf{I}(z_G)$ and $c_0\,\mathbf{Z}_C\,\mathbf{Q}(z_H)$, respectively. Thus, for $\mathbf{I}(z_G) = c_0\,\mathbf{Q}(z_H)$ we have $\psi_G(x, y) = \psi_H(x, y)$, so that (9) and (17) show that $\rho_S/\varepsilon_0 = \eta_0 j_S$. Consequently,

$$\mathbf{N}(x, y) = \mathbf{M}(x, y) \quad (22)$$

Thus, we obtain the following theorem.

Theorem on the connection of charge and current densities. For an MTL with small resistive losses (h.f. current distribution), at a given abscissa z, for a given $\mathbf{I}(z)$, the surface current density j_S at the surface of the conductors is the product of an arbitrary velocity v_D and the surface charge density at the surface of the conductors in a configuration where all dielectrics are replaced by vacuum and where $\mathbf{Q}(z) = \mathbf{I}(z)/v_D$.

Let us now see how this theorem can be used to easily determine the h.f. current distribution. The MTL model of the
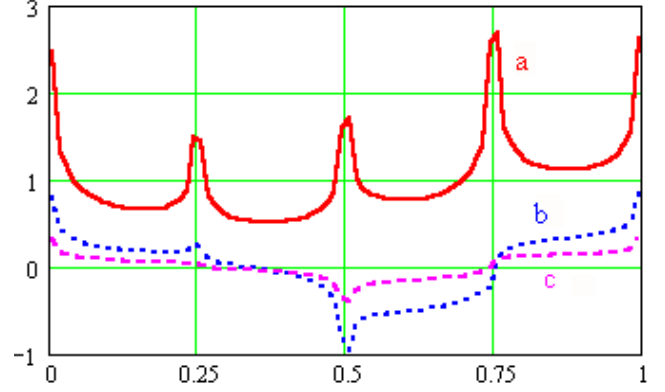
Fig. 2. Surface current density (arbitrary unit) measured on TC 1, versus s, when a current is injected in the TC 1 (a), TC 2 (b) or TC 3 (c).

interconnection includes the h.f. p.u.l. external inductance matrix of the interconnection 1, denoted by $\mathbf{L}_0$. This matrix is given by $\mathbf{L}_0 = \mu_0\,\varepsilon_0\,\mathbf{C}_0^{-1}$, where μ_0 is the permeability of vacuum and $\mathbf{C}_0$ is the p.u.l. capacitance matrix of the interconnection 2. In order to assess $\mathbf{C}_0$, the perimeter of each TC is usually divided in small strips. Let us use A to denote the set of the indices of the strips which form the boundaries of all TCs. The set A may be partitioned into mutually exclusive subsets $A_1, \dots A_n$, where for any integer j such that $1 \le j \le n$, the subset A_j contains the indices of the strips of the TC number j. At the final stage of the computation of $\mathbf{C}_0$ by the method of moment using pulse expansion and point matching [7, § 3.3], a capacitance matrix $\mathcal{C}_0$ is computed, an entry $\mathcal{C}_{0\,\alpha\beta}$ of $\mathcal{C}_0$ being the p.u.l. charge of the strip number α when the voltage between the center of the strip number β and ground is 1 V, the voltage between the center of each other strip and ground being 0 V. The entry $C_{0\,ij}$ of $\mathbf{C}_0$ is given by

$$C_{0\,ij} = \sum_{\alpha\in A_i}\sum_{\beta\in A_j}\mathcal{C}_{0\,\alpha\beta} \quad (23)$$

At this point, an estimate of $\mathbf{N}(x, y) = \mathbf{M}(x, y)$ is available, since, at any point (X, Y) on the strip number α we have

$$\mathbf{N}(X,Y) \approx \frac{1}{w_\alpha}\sum_{j=1}^{n}\left(\sum_{\beta\in A_j}\mathcal{C}_{0\,\alpha\beta}\right)^t\mathbf{e}_j\mathbf{C}_0^{-1} \quad (24)$$

where we use w_α to denote the width of the strip α, where $^t\mathbf{A}$ denotes the transpose of $\mathbf{A}$ and where $\mathbf{e}_j$ denotes the column-vector having n entries, said entries being zero except the j-th entry which is equal to 1. Let us for instance consider the interconnection shown in Fig. 1, with $t = w_1 = w_2 = 50$ µm and $h = d_1 = d_2 = 50$ µm. On a given TC, the normalized arc length along the perimeter of the cross section increases clockwise, from the point $s = 0$, shown in Fig. 1, to $s = 1$. The Fig. 2 shows the current distribution on the TCs when a current is injected on a single TC, computed using (24) and 336 matching points. Current crowding is visible near edges. The proximity effect is also plain. Thus, eddy currents are induced in all non-excited conductors, and this phenomenon will contribute to the h.f. resistive losses.

VI. High-frequency P.U.L. Resistance Matrix

Let us assume that we inject the currents of the column-vector $\mathbf{I}$ into the TCs. Let us use $i_S(\alpha, \mathbf{I})$ to denote the current flowing in the strip α. For any j, we have

$$\sum_{\alpha \in A_j} i_S(\alpha, \mathbf{I}) = [\mathbf{I}]_j \qquad (25)$$

where $[\mathbf{x}]_j$ is the j-th entry of the vector $\mathbf{x}$. At high frequencies, according to the theorem on the surface current density, we may define a real matrix $\mathbf{Q}_V$ having n columns such that, for any $\mathbf{I}$, the current flowing in the strip α is given by

$$i_S(\alpha, \mathbf{I}) = k[\mathbf{Q}_V \, \mathbf{I}]_\alpha \qquad (26)$$

where k is an arbitrary non-zero constant. Using (25), we get

$$i_S(\alpha, \mathbf{I}) = \sum_{j=1}^{n} \frac{Q_{V\alpha j} I_j}{\sum_{\beta \in A_j} Q_{V\beta j}} \qquad (27)$$

where the $Q_{V\alpha j}$ are the entries of $\mathbf{Q}_V$. Let us assume that the resistivity and the skin depth are the same in all TCs and denoted by ρ_{TC} and δ_{TC}, respectively. At sufficiently high frequencies, the thickness and width of each TC are each much greater than δ_{TC}. The surface current density being homogeneous over each strip, the p.u.l. power dissipated in the TCs is

$$P_{TC} = \frac{\rho_{TC}}{\delta_{TC}} \sum_{\alpha \in A} \frac{|i_S(\alpha, \mathbf{I})|^2}{w_\alpha} \qquad (28)$$

The h.f. p.u.l. resistance matrix of the TCs, denoted by $\mathbf{R}_{HFTC}$, is defined by $P_{TC} = \mathbf{I}^* \mathbf{R}_{HFTC} \mathbf{I}$, where $\mathbf{I}^*$ denotes the hermitian adjoint of $\mathbf{I}$. Using (27) and (28), we may easily show that

$$\mathbf{R}_{HFTC} = \frac{\rho_{TC}}{\delta_{TC}} \mathbf{K}_{TC} \qquad (29)$$

where we refer to $\mathbf{K}_{TC}$ as the matrix of the equivalent inverse widths of the TCs, the entries of $\mathbf{K}_{TC}$ being given by

$$K_{TCij} = \frac{1}{\left(\sum_{\beta \in A_i} Q_{V\beta i}\right)\left(\sum_{\beta \in A_j} Q_{V\beta j}\right)} \sum_{\alpha \in A} \frac{Q_{V\alpha i} Q_{V\alpha j}}{w_\alpha} \qquad (30)$$

At this stage, the theorem on the connection of charge and current densities can be used to obtain $\mathbf{Q}_V$, since it tells us that we may define $Q_{V\alpha i}$ as the p.u.l. electrostatic charge on the strip α when the p.u.l charge of the TC number i is 1, the p.u.l. charge on each other TC being zero. In other words, we can use

$$Q_{V\alpha i} = \sum_{j=1}^{n} \left(\sum_{\beta \in A_j} \mathcal{C}_{0\alpha\beta}\right){}^t \mathbf{e}_j \mathbf{C}_0^{-1} \mathbf{e}_i \qquad (31)$$

A similar reasoning can be used to obtain the h.f. p.u.l. resistance matrix of the GC, denoted by $\mathbf{R}_{HFGC}$, defined by $P_{GC} = \mathbf{I}^* \mathbf{R}_{HFGC} \mathbf{I}$, where P_{GC} is the p.u.l. power dissipated in the GC. Using ρ_{GC} and δ_{GC} to denote the resistivity and the skin depth of the GC, respectively, we find

$$\mathbf{R}_{HFGC} = \frac{\rho_{RC}}{\delta_{RC}} \mathbf{K}_{GC} \qquad (32)$$

where we refer to $\mathbf{K}_{GC}$ as the matrix of the equivalent inverse widths of the GC, the entries of $\mathbf{K}_{GC}$ being given by

$$K_{GCij} = \frac{\int_C \{\mathbf{n} \cdot \mathbf{E}_i(\xi)\}\{\mathbf{n} \cdot \mathbf{E}_j(\xi)\} d\xi}{\left(\int_C \mathbf{n} \cdot \mathbf{E}_i(\xi) d\xi\right)\left(\int_C \mathbf{n} \cdot \mathbf{E}_j(\xi) d\xi\right)} \qquad (33)$$

where ξ is an arc length on the boundary of the GC and where $\mathbf{n} \cdot \mathbf{E}_i(\xi)$ is the electrostatic field component normal to the surface of the GC when the p.u.l. charge of each strip is given by (31), the integration path C extending over the boundary of the GC.

The conductors being reciprocal and passive, $\mathbf{K}_{TC}$ and $\mathbf{K}_{GC}$ are frequency-independent real positive semidefinite matrices [9, § 7.1]. Thus, any diagonal entry of $\mathbf{K}_{TC}$ or $\mathbf{K}_{GC}$ is non-negative. As an example, for the multiconductor microstrip interconnection considered in Section V, using 336 matching points, we find

$$\mathbf{K}_{TC} = \begin{pmatrix} 6961 & 806 & 88 & 0 \\ 806 & 7466 & 985 & 88 \\ 88 & 985 & 7466 & 806 \\ 0 & 88 & 806 & 6961 \end{pmatrix} \mathrm{m}^{-1} \qquad (34)$$

In (34), all entries of $\mathbf{K}_{TC}$ are nonnegative. However, for other interconnections, we have obtained negative non-diagonal entries in $\mathbf{K}_{TC}$. In all configurations for which we have computed $\mathbf{K}_{TC}$ and $\mathbf{K}_{GC}$, we found that $\mathbf{K}_{TC}$ is strictly diagonally dominant [9, § 6.1.9], and that $\mathbf{K}_{GC}$ is nonnegative [9, § 8.1].

VII. A Model for the P.U.L. Impedance Matrix

In this paper, the p.u.l. internal impedance matrix of the interconnection, denoted by $\mathbf{Z}_I$, is given by $\mathbf{Z}_I = \mathbf{Z} - j\omega \mathbf{L}_0$, where $\mathbf{Z}$ is the p.u.l. impedance matrix of the interconnection. This definition is not the one used in [2], but it is in line with the one used in [10, § 2.8]. We clearly have $\mathbf{Z}_I = \mathbf{0}$ for lossless conductors.

Complying with Wheeler's incremental-inductance rule [11], we assume that, for frequencies high enough for the skin effect to be well developed, the real and imaginary parts of $\mathbf{Z}_I$ become approximately equal and exhibit a $f^{1/2}$ increase with frequency. Thus, the h.f. p.u.l. internal impedance matrix satisfies

$$\mathbf{Z}_{IHF} \approx (1 + j)\left(\frac{\rho_{TC}}{\delta_{TC}} \mathbf{K}_{TC} + \frac{\rho_{RC}}{\delta_{RC}} \mathbf{K}_{RC}\right) \qquad (35)$$

Wheeler's incremental-inductance rule is not an exact law, but it gives reasonably accurate values for a single conductor [2] [12].

Some authors assume that, in the Laplace domain, $\mathbf{Z}_I$ is given by the model $\mathbf{Z}_S = \mathbf{A} + s^{1/2} \mathbf{B}$ where s is the Laplace transform variable and where $\mathbf{A}$ and $\mathbf{B}$ are two frequency independent matrices [7, § 5.3]. $\mathbf{A}$ and $\mathbf{B}$ can be determined such that $\mathbf{Z}_S$ complies with (35) and provides an exact dc resistance matrix. However, $\mathbf{Z}_S$ produces non-physical infinite dc self-inductances and infinite or zero dc mutual inductances. Also, in the case of a

single TC of circular cross-section having a coaxial return path, for $s = j\omega$ where ω is real, the model $Z_S = A + B\,s^{1/2}$ produces large errors in the vicinity of the skin-effect onset frequency [10, § 2.8].

In the same case of a single TC of circular cross-section having a coaxial return path, another model assumes that $\mathbf{Z}_I$ is given by $Z_B = (A + B\,s)^{1/2}$. This model is also compatible with (35) and it can provide a good approximation of the exact solution at all frequencies [10, § 2.8]. The accuracy of Z_B in the case of the circular symmetry is caused by the fact that A and B can be chosen such that an exact h.f. impedance, an exact dc resistance and an exact dc inductance are simultaneously obtained. Unfortunately, this miracle does not occur with other single-TC configurations (for instance a TC having a rectangular cross-section) and this model using Z_B does not lend itself to an obvious generalization to $n \geq 2$.

We have tried to define a p.u.l. internal impedance matrix model combining the following properties: being exact at dc; complying with (35); producing finite and reasonable dc self- and mutual inductances; and ensuring passivity. For want of a better approach, we have used a trial-and-failure process in which the most difficult part was the proof of passivity covered in Section VIII. This led us to a new model for $\mathbf{Z}_I$, denoted by $\mathbf{Z}_N$ and defined by

$$\mathbf{Z}_N = \mathbf{Z}_{NR} + \mathbf{Z}_{NTC} + \mathbf{Z}_{NGC} \qquad (36)$$

where, for the indices α and β ranging from 1 to n with $\alpha \neq \beta$, the entries of the matrices $\mathbf{Z}_{NR}$, $\mathbf{Z}_{NTC}$ and $\mathbf{Z}_{NGC}$ are respectively given by

$$\begin{cases} Z_{NR\alpha\alpha} = R_{DC\alpha} + R_{DCGC} \\[2ex] Z_{NR\alpha\beta} = \dfrac{R_{DCGC}}{\sqrt{1 + \dfrac{4sL_{MAXGC}^2}{\mu_0 \rho_{GC} \left(\max\limits_{1 \leq i \leq n} K_{GCii} \right)^2}}} \end{cases} \qquad (37)$$

$$\begin{cases} Z_{NTC\alpha\alpha} = \dfrac{\mu_0 \rho_{TC} K_{TC\alpha\alpha}^2}{2 L_{MAX\alpha}} \left(\sqrt{1 + \dfrac{4sL_{MAX\alpha}^2}{\mu_0 \rho_{TC} K_{TC\alpha\alpha}^2}} - 1 \right) \\[4ex] Z_{NTC\alpha\beta} = \dfrac{\mu_0 \rho_{TC} K_{TC\alpha\beta} \left(\sqrt{1 + \dfrac{4s}{\mu_0 \rho_{TC}} \left(\min\left\{ \dfrac{L_{MAX\alpha}}{K_{TC\alpha\alpha}}, \dfrac{L_{MAX\beta}}{K_{TC\beta\beta}} \right\} \right)^2} - 1 \right)}{2 \min\left\{ \dfrac{L_{MAX\alpha}}{K_{TC\alpha\alpha}}, \dfrac{L_{MAX\beta}}{K_{TC\beta\beta}} \right\}} \end{cases} \qquad (38)$$

and

$$\mathbf{Z}_{NGC} = \dfrac{\mu_0 \rho_{GC} \max\limits_{1 \leq i \leq n} K_{GCii}}{2 L_{MAXGC}} \left(\sqrt{1 + \dfrac{4sL_{MAXGC}^2}{\mu_0 \rho_{GC} \left(\max\limits_{1 \leq i \leq n} K_{GCii} \right)^2}} - 1 \right) \mathbf{K}_{GC} \qquad (39)$$
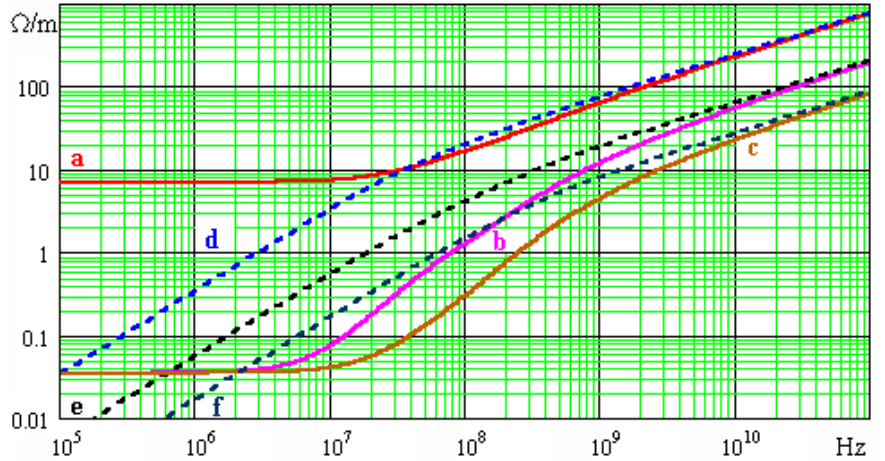
Fig. 3. Some entries of $\mathbf{Z}_N$ versus frequency. Curve a: real part of $Z_{N\,11}$. Curve b: real part of $Z_{N\,12}$. Curve c: real part of $Z_{N\,13}$. Curve d: imaginary part of $Z_{N\,11}$. Curve e: imaginary part of $Z_{N\,12}$. Curve f: imaginary part of $Z_{N\,13}$.

where each square root symbol denotes the principal root, where the p.u.l. dc resistances of the TCs are denoted by $R_{DC\,1}$ to $R_{DC\,n}$, the p.u.l. dc resistance of the GC is denoted by R_{DCGC}, the p.u.l. inductances $L_{MAX\,1}$ to $L_{MAX\,n}$ relate to the TCs and the p.u.l. inductance L_{MAXGC} relates to the GC.

Since it comprises several terms in the form $(A + B\,s)^{1/2}$, the model $\mathbf{Z}_N$ can be seen as an extension of Z_B, intended to provide a causal and passive approximation for any configuration of the TCs and GC.

The Fig. 3 shows some entries of $\mathbf{Z}_N$ computed with (36)-(39), for the multiconductor microstrip interconnection considered in Section V. In this computation, $L_{MAX\,1}$ to $L_{MAX\,n}$ are equal to the p.u.l. dc internal inductance $L_{DC} = 43.8$ nH/m of the identical TCs, computed using a closed-form approximation [13, eq. (30)-(31)]. In this computation, $L_{MAXGC} = L_{DC}/10$. In Fig. 3, we also assume $\rho_{GC} = \rho_{TC} = 17.24$ nΩ.m and $R_{DCGC} = 0.034$ Ω/m. We find that the dc internal inductance matrix is given by

$$\lim_{\omega \to 0} \frac{\text{Im}\big(\mathbf{Z}_N(j\omega) \big)}{\omega} = \begin{pmatrix} 53.1 & 8.7 & 2.6 & 1.2 \\ 8.7 & 52.9 & 9.8 & 2.6 \\ 2.6 & 9.8 & 52.9 & 8.7 \\ 1.2 & 2.6 & 8.7 & 53.1 \end{pmatrix} \frac{\text{nH}}{\text{m}} \qquad (40)$$

We observe that $\mathbf{Z}_N$ produces finite and reasonable dc self- and mutual inductances. This is in contrast with the model $\mathbf{Z}_S$, in which infinite dc self- and mutual inductances produce various artifacts, which are not easy to detect and sort out in time domain simulations. It can easily be shown that our model has the following characteristics:

■ $\mathbf{Z}_N$ is exact at dc;
■ $\mathbf{Z}_N$ complies with (35) at frequencies sufficiently high to allow us to neglect the 1 in each square root of (38)-(39) and to neglect $\mathbf{Z}_{NR}$ in (36);
■ the dc internal inductance produced by $Z_{N\,\alpha\,\alpha}$ ranges between $L_{MAX\,\alpha}$ and $L_{MAX\,\alpha} + L_{MAXGC}$ and, for $\alpha \neq \beta$, the dc internal inductance produced by $Z_{N\,\alpha\,\beta}$ is finite.

VIII. PASSIVITY OF THE MODEL

We shall outline the proof of the passivity of our model $\mathbf{Z}_N$, based on the following well-known theorem [3, § IV.D] [4].

Theorem on passivity. An impedance matrix $\mathbf{Z}(s)$ represents a passive linear system if and only if

(*i*) each entry of $\mathbf{Z}(s)$ is defined and analytic in the half plane $\sigma > 0$, where $\sigma = \text{Re}(s)$;

(*ii*) $\mathbf{Z}^*(s) + \mathbf{Z}(s)$, where the star indicates the hermitian adjoint, is a positive semidefinite matrix for all s such that $\sigma > 0$;

(*iii*) $\mathbf{Z}(\overline{s}) = \overline{\mathbf{Z}}(s)$, where the bar indicates the complex conjugate.

The conditions (*i*) and (*iii*) are clearly satisfied for the impedance matrices $\mathbf{Z}_N$, $\mathbf{Z}_{NR}$, $\mathbf{Z}_{NTC}$ and $\mathbf{Z}_{NGC}$ defined by (36)-(39). The condition (*ii*) is addressed below.

If r and $m_1, ..., m_n$ are real numbers, for any $p \in \{1,..., n\}$ let us use $\mathbf{M}_p(m_1, ..., m_p)$ to denote the matrix

$$\mathbf{M}_p\left(m_1, \cdots, m_p\right) = \begin{pmatrix} m_1 & r & \cdots & r \\ r & \ddots & \ddots & \vdots \\ \vdots & \ddots & \ddots & r \\ r & \cdots & r & m_p \end{pmatrix} \quad (41)$$

If for all $\alpha \in \{1,..., n\}$ we have $m_\alpha > r > 0$, we can prove inductively that, for any $p \in \{1,..., n\}$, we have

$$\det\left(\mathbf{M}_p\left(m_1, \cdots, m_p\right)\right) > 0 \quad (42)$$

so that, all elements of a nested chain of n principal minors being positive, $\mathbf{M}_n(m_1, ..., m_n)$ is positive definite by [9, § 7.2.5]. A diagonal entry of $\mathbf{Z}_{NR} + \mathbf{Z}_{NR}*$ is given by

$$Z_{NR\alpha\alpha} + \overline{Z}_{NR\alpha\alpha} = 2\left(R_{DC\alpha} + R_{DCGC}\right) \quad (43)$$

This quantity is positive. A non-diagonal entry of $\mathbf{Z}_{NR} + \mathbf{Z}_{NR}*$ is given by

$$Z_{NR\alpha\beta} + \overline{Z}_{NR\beta\alpha} = \frac{R_{DCGC}}{\sqrt{1+sE}} + \frac{R_{DCGC}}{\sqrt{1+\overline{s}E}} \quad (44)$$

where $\alpha \neq \beta$ and where E is a positive real number. We see that $\mathbf{Z}_{NR} + \mathbf{Z}_{NR}*$ is in the form of (41), and it is possible to prove that, if $\sigma > 0$, then for all $\alpha \in \{1,..., n\}$, we have $m_\alpha > r > 0$. Thus, we conclude that the condition (*ii*) is satisfied by $\mathbf{Z}_{NR}$.

$\mathbb{R}_+\backslash\{0\}$ being the set of positive real numbers, let us define a function of $s \in \mathbb{C}$ and $\lambda \in \mathbb{R}_+\backslash\{0\}$, by

$$z(s,\lambda) = \frac{c}{2\lambda}\left(\sqrt{1+\frac{4s\lambda^2}{c}} - 1\right) \quad (45)$$

where $c \in \mathbb{R}_+\backslash\{0\}$. $z(s, \lambda)$ appears 3 times in (38)-(39). It can be shown that:

(*iv*) for $\sigma > 0$, we have $\text{Re}(z(s, \lambda)) > 0$;

(*v*) for $\sigma > 0$, $\text{Re}(z(s, \lambda))$ is an increasing function of λ.

Using (*v*) and the assumption that $\mathbf{K}_{TC}$ is strictly diagonally dominant (see the end of Section VI), it is possible to show that if $\sigma > 0$ then $\mathbf{Z}_{NTC} + \mathbf{Z}_{NTC}*$ is strictly diagonally dominant. Each $K_{TC\alpha\alpha}$ being positive, by (*iv*) each diagonal entry of $\mathbf{Z}_{NTC} + \mathbf{Z}_{NTC}*$ is positive for $\sigma > 0$. We conclude that, if $\sigma > 0$ then $\mathbf{Z}_{NTC} + \mathbf{Z}_{NTC}*$ is positive definite by [9, § 7.2.3]. Thus, the condition (*ii*) is satisfied by $\mathbf{Z}_{NTC}$.

By (*iv*), if $\sigma > 0$, $\mathbf{Z}_{NGC} + \mathbf{Z}_{NGC}*$ is the product of a positive constant and the positive definite matrix $\mathbf{K}_{GC}$, so that $\mathbf{Z}_{NGC} + \mathbf{Z}_{NGC}*$ is positive definite by [9, § 7.1.3] and the condition (*ii*) is satisfied by $\mathbf{Z}_{NGC}$. Moreover, since

$$\mathbf{Z}_N + \mathbf{Z}_N^* = \mathbf{Z}_{NR} + \mathbf{Z}_{NR}^* + \mathbf{Z}_{NTC} + \mathbf{Z}_{NTC}^* + \mathbf{Z}_{NGC} + \mathbf{Z}_{NGC}^* \quad (46)$$

we find that $\mathbf{Z}_N + \mathbf{Z}_N*$ is positive definite for $\sigma > 0$. Thus, the condition (*ii*) is satisfied by $\mathbf{Z}_N$. We conclude that the impedance matrices $\mathbf{Z}_N$, $\mathbf{Z}_{NR}$, $\mathbf{Z}_{NTC}$ and $\mathbf{Z}_{NGC}$ each represents a passive linear system, and consequently a causal system [3, § III.C] [4].

IX. CONCLUSION

We have introduced a new technique to compute the h.f. current distribution in a multiconductor interconnection. It takes into account the crowding of currents at the edges of a conductor (edge effect), and the influence of other conductors (proximity effect). For conductors having an homogeneous resistivity, we have used this technique to compute the frequency-independent $\mathbf{K}_{TC}$ and $\mathbf{K}_{GC}$ which are used to obtain $\mathbf{R}_{HFTC}$ and $\mathbf{R}_{HFGC}$.

We have defined a new model for the p.u.l. internal impedance matrix. This analytical model is physically reasonable and realizable in the sense that it is exact at dc, accurate at high frequencies, corresponds to a finite dc inductance matrix, and that it represents a causal and passive linear system. As far as we know, no other analytical model combines these properties.

REFERENCES

[1] A. Cangellaris, "A Note on the calculation of the current distribution in lossy microstrip structures", *IEEE Microwave Guided Wave Lett.*, Vol. 1, No. 4, April 1991, pp. 81-83.

[2] A. Rong, A.C. Cangellaris, "Note on the definition and calculation of the per-unit-length internal impedance of a uniform conducting wire", *IEEE Trans. Electromagn. Compat.*, vol. 49, No. 3, August 2007, pp. 677-681.

[3] P. Triverio, S. Grivet-Talocia, M.S. Nakhla, F.G. Canavero and R. Achar, "Stability, causality and passivity in electrical interconnect models", *IEEE Trans. on Advanced Packaging*, vol. 30, No. 7, November 2007, pp. 795-808.

[4] A.H. Zemanian, "An N-port realizability theory based on the theory of distributions", *IEEE Trans. Circuit Theory*, vol. 10, No. 2, pp. 265-274, June 1963.

[5] C.T.A. Johnk, *Engineering Electromagnetic Fields and Waves*, John Wiley & Sons, 1975.

[6] R.E. Collin, *Field Theory of Guided Waves*, 2nd ed., IEEE Press, 1991.

[7] C.R. Paul, *Analysis of Multiconductor Transmission Lines*, John Wiley & Sons, 1994.

[8] F. Broydé and E. Clavelier, "A new method for the reduction of crosstalk and echo in multiconductor interconnections", *IEEE Trans. Circuits Syst. I*, vol. 52, No. 2, pp. 405-416, Feb. 2005.

[9] R.A. Horn, C.R. Johnson, *Matrix analysis*, Cambridge University Press, 1985.

[10] H. Johnson and M. Graham, *High-Speed Signal Propagation — Advanced Black Magic*, Prentice Hall PTR, 2003.

[11] H.A. Wheeler, "Formulas for the Skin Effect", *Proceedings of the IRE*, vol. 30, No. 9, Sept. 1942, pp. 412-424.

[12] G. Antonini, A. Orlandi and C.R. Paul, "Internal Impedance of Conductors of Rectangular Cross Section", *IEEE Trans. on Microwave Theory Tech.*, vol. 47, No. 7, July 1999, pp. 979-985.

[13] C.L. Holloway and E.F. Kuester, "DC Internal Inductance for a Conductor of Rectangular Cross Section", *IEEE Trans. Electromagnetic Compatibility*, vol. 51, No. 2, May 2009, pp. 338-344.